



Proper fraction of inspired oxygen for reduction of oxygen-induced canine cerebrospinal fluid hyperintensity on fluid attenuation inversion recovery sequence using low-field magnetic resonance imaging

Moonjung JANG¹, Jaewoo HWANG¹, Jihye NAM¹, Dalhae KIM¹,
Wongyun SON¹, Inhyung LEE¹, Mincheol CHOI¹ and Junghee YOON¹*

¹College of Veterinary Medicine and the Research Institute for Veterinary Science, Seoul National University, Seoul 08826, Republic of Korea

ABSTRACT. Oxygen-induced cerebrospinal fluid (CSF) hyperintensity artifact is inevitable in fluid attenuation inversion recovery (FLAIR) magnetic resonance (MR) images of anesthetized animals. This experimental study aimed to confirm the occurrence of this artifact on low-field magnetic resonance imaging (MRI), and to determine the fraction of inspired oxygen (FiO₂) that is safe and does not induce this artifact in canine brain MRI. Six healthy dogs underwent brain FLAIR MR scans under general anesthesia with 21%, 30%, 50%, 70%, and 100% FiO₂. The signal intensity (SI) ratio was calculated as the SI of CSF spaces divided by that of normalizing regions. The SI ratios of 21% FiO₂ images were significantly different from those of 100% FiO₂ images, indicating the presence of artifacts on 100% FiO₂ images. The SI ratios of 30% FiO₂ images were not significantly different from those of 21% FiO₂ images for any of CSF spaces. However, they were significantly different from those of 100% FiO₂ images in the cerebral sulci, third ventricle, interpeduncular cistern, mesencephalic aqueduct, and subarachnoid space at the level of the first cervical vertebra ($P < 0.05$). All dogs had normal partial pressure of arterial oxygen (PaO₂) during inhalation of 30% FiO₂, while two dogs had low PaO₂ during inhalation of 21% FiO₂. Our findings support the hypothesis that high FiO₂ induces CSF hyperintensity artifact on low-field FLAIR MR images in dogs. FiO₂ of 30% is appropriate for obtaining brain FLAIR MR images with fewer artifacts in dogs.

KEY WORDS: cerebrospinal fluid, fluid attenuation inversion recovery, fraction of inspired oxygen, hyperintensity artifact, magnetic resonance imaging

J. Vet. Med. Sci.
82(9): 1321–1328, 2020
doi: 10.1292/jvms.20-0060

Received: 3 February 2020
Accepted: 9 July 2020
Advanced Epub:
20 July 2020

Brain magnetic resonance imaging (MRI) is a useful diagnostic tool for various intracranial diseases [6, 15, 20]. T2-weighted fluid attenuation inversion recovery (FLAIR) sequence is one of the essential sequences for human and veterinary brain MRI protocols [16, 18]. It is utilized to identify the lesions located adjacent to the cerebrospinal fluid (CSF) spaces, such as the ventricles, because it uses an inversion time to null the CSF signal [6, 18]. Hyperintensity of CSF spaces on FLAIR images can be observed in pathologic conditions such as increased protein content or cellularity, hemorrhage, infection, and leptomeningeal seeding metastasis. However, hyperintensity may also result from the presence of artifacts such as CSF pulsation, magnetic susceptibility artifact, truncation, and motion artifact [6, 8, 18, 19].

Unexpected CSF hyperintensity on FLAIR images has been observed in anesthetized human patients, and several studies have revealed supplemental oxygen to be the cause of the artifact [1, 3–5]. Increased partial pressure of oxygen in the CSF ($P_{\text{CSF}O_2}$) decreases the T1 relaxation time owing to paramagnetic property of oxygen, and incomplete signal suppression occurs in the CSF spaces. Furthermore, several studies have investigated this phenomenon with respect to the difference in the degree of artifact depending on the method of oxygen supply or the concentration of supplied oxygen, the time at which the hyperintensity begins to occur after initiation of oxygen supply, and experiments on healthy volunteers [1, 3–5, 18].

A recent prospective study identified oxygen-induced hyperintensity artifact in the CSF of dogs and cats using a 1.0 T magnetic resonance (MR) scanner [14]. Acquiring an understanding of this artifact is important in veterinary medicine because the use of general anesthesia with respiratory anesthetic agents and oxygen is unavoidable while performing brain MRI in dogs and cats.

*Correspondence to: Yoon, J.: heeyoon@snu.ac.kr

©2020 The Japanese Society of Veterinary Science



This is an open-access article distributed under the terms of the Creative Commons Attribution Non-Commercial No Derivatives (by-nc-nd) License. (CC-BY-NC-ND 4.0: <https://creativecommons.org/licenses/by-nc-nd/4.0/>)

Although many studies have investigated this artifact with the use of a high-field MR scanner, a study with a low-field MR scanner is required, since they are currently in wide use in veterinary practice [1, 3–5, 12, 14]. We hypothesized that oxygen-induced artifact would occur in FLAIR images obtained using a low-field MR scanner, and that there would be a threshold fraction of inspired oxygen (FiO_2) level that would induce an identifiable artifact. The aim of this experimental study was to confirm the occurrence of oxygen-induced CSF hyperintensity artifact on FLAIR MR images obtained using a low-field MR scanner, and to determine the appropriate FiO_2 value that does not induce this artifact, while at the same time maintaining a safe partial pressure of arterial oxygen (PaO_2).

MATERIALS AND METHODS

Animals

This study was an experimental study design. The experiments were performed based on guidelines of the Institutional Animal Care and Use Committee. Six healthy adult beagles, including two females and four males, were included and decisions for inclusion were made by two veterinarians with two years of diagnostic imaging experience. The age range was 19–60 months (mean, 41.17; standard deviation [SD], ± 20.71), and body weight was 9.6–14.9 kg (mean, 12.47 kg; SD, ± 2.26); physical examination, complete blood count, and serum chemistry of all dogs did not reveal any abnormal signs. The dogs with intracranial abnormality found in MRI scan were excluded from the study.

MR scanning technique

MR scanning and anesthesia monitoring were performed by one author. All dogs were fasted for 12 hr before administering general anesthesia for MR scans. The dogs were sedated with acepromazine (0.01 mg/kg IV, Sedaject[®], Samu Median Co., Seoul, South Korea), and general anesthesia was induced by alfaxalone (2 mg/kg IV, Alfaxan[®] Jurox Pty Ltd., Rutherford, NSW, Australia), and maintained using isoflurane (Ifiran[®], Hana Pharm., Seoul, South Korea) in 21% FiO_2 via an endotracheal tube. FiO_2 was manually regulated by two flowmeters, each providing room air and 100% oxygen. MR scans were performed using a 0.3 T permanent MR scanner (Hitachi AIRIS Vento, Hitachi Medical Co., Tokyo, Japan).

During MRI, the patients were ventilated with a mechanical system (Multiplus[®], Royal Medical Co., Ltd., Pyeongtaek, Korea) and the heart rate, respiratory rate, blood pressure, FiO_2 , end tidal carbon dioxide concentration, blood peripheral capillary oxygen saturation, and minimum alveolar concentration were continuously monitored and recorded every 5–15 min. A 24-G intravascular catheter (Bio-safety I.V Catheter V4712-024-075, Sewoon Medical Co., Ltd., Cheonan, Korea) was inserted at the dorsal pedal artery for invasive blood pressure monitoring and arterial blood sampling for blood gas analysis. Glycopyrrolate (5 $\mu\text{g}/\text{kg}$ IV, Morbinul[®], Myungmoon Pharm Co., Ltd., Seoul, Korea) was on hand to be administered in case of hypotension.

The first transverse and sagittal FLAIR sequence imaging was performed with 21% FiO_2 . The FiO_2 was adjusted to 30% after the first scan, and the adjusted gas was supplied for at least 10 min for equilibration. Body temperature measurement and arterial blood sampling were performed after 10 min, and the next scan was initiated. Arterial blood analysis was performed using a blood gas analyzer (ABL80 FLEX[®], Radiometer, Copenhagen, Denmark) immediately after the sampling with an arterial blood collection syringe (BD Preset[™], Becton, Dickinson and Co., Plymouth, UK). Same procedures were performed before each scan with all next FiO_2 levels: 50%, 75%, and 100%. CSF centesis was performed in the cerebellomedullary cistern after all scans were completed for each dog. Moreover, CSF analysis was performed within 1 hr of sampling. The scan parameters were as follows: repetition time (TR)=11,635 msec, echo time (TE)=120 msec, flip angle=90, number of acquisition (NEX)=2, slice thickness=3.00 mm, slice interval=3.30 mm, field of view (FOV)=190 \times 190 mm, matrix=256 \times 212, scan duration=8 min and 9 sec. for transverse plane, and TR=11,420 msec, TE=104 msec, flip angle=90, NEX=2, slice thickness=3.00 mm, slice interval=3.30 mm, FOV=190 \times 190 mm, matrix=256 \times 212, scan duration=10 min and 6 sec for sagittal plane.

Image analyses

Three authors who have experience in diagnostic imaging participated in the data recording and analyses. The acquired MR images were stored in the JPEG format and then transferred to a computer for analysis using a public domain image processing program (ImageJ, US National Institutes of Health, <https://imagej.nih.gov/ij/>) for measuring the signal intensity (SI) of the CSF spaces and the regions for normalization. The following CSF spaces were assessed: 3 cerebral sulci, third ventricle, fourth ventricle, interpeduncular cistern, mesencephalic aqueduct, subarachnoid space at the C1 vertebral level in transverse images, and fourth ventricle in midline sagittal images. The following regions were assessed for normalization: white matter of gyri adjacent to the sulci CSF, thalamus, pons, cerebral peduncle, and spinal cord at the first cervical vertebra (C1) level. These regions were used for normalization of the corresponding CSF spaces in the same image.

Criteria to choose slice, shape and size of ROI are as follows. Three different sulci with homogeneously hypointense CSF signal in FiO_2 21% images were selected in consensus from two observers. The locations of three sulci were different in each dog; selected sulci include the Lt. and Rt. coronal groove, Lt. and Rt. splenial groove, caudal and middle suprasylvian groove, and marginal groove. A linear ROI was drawn to include one sulcus and gray mater besides. SI values of the cerebral sulci were acquired using the plot profiles. As the linear plot profile includes the two gray mater layers besides the sulci, the average of the two lowest values among the whole plot profile were used as the SI values of the cerebral sulci. For the other CSF spaces, slices which has the largest area of each CSF spaces were chosen. Observers respectively drew the ROI of the CSF spaces along the margin by hand, and drew the ROI of the normalizing region in shape of the largest circle that can be drawn in the region. SI

values of CSF spaces other than three sulci and the normalizing regions were the average of SI values in each ROI. For sulci CSF spaces, the mean value of the three SI ratios was used for statistical assessment. This measurement was independently performed by two authors twice each to obtain four data sets; the observers were blinded to each other's measurements. The observers drew the regions of interest (ROI) on the 21% FiO₂ images of each CSF spaces because those had the most distinct margin of CSF spaces among images of other FiO₂ levels (Fig. 1). The same ROI that were set in the images of 21% FiO₂ were applied to the images of other FiO₂ levels. Heterogeneity of SI in each ROI has not been considered.

The SI ratio was calculated as the SI value of CSF spaces divided by the SI value of the normalizing regions. The calculation was performed by one author with expertise in diagnostic imaging. Before calculating the SI ratio of the CSF spaces, the SI value of the white matter, thalamus, pons, cerebral peduncle, and spinal cord was divided by the SI value of the white matter, which is not affected by oxygen [3], in order to assess whether the values are suitable for normalization. The cerebral sulcus to the white matter, third ventricle to the thalamus, fourth ventricle (both transverse and sagittal plane) to the pons, interpeduncular cistern to the cerebral peduncle, mesencephalic aqueduct to cerebral peduncle, and C1 subarachnoid space to spinal cord SI ratios were calculated based on the SI values.

A subjective evaluation of the artifact grade in the general CSF spaces was performed by an author with expertise in diagnostic imaging using DICOM workstation (INFINITT PACS®, INFINITT Healthcare Co., Ltd., Seoul, Korea). FLAIR image series (transverse and sagittal planes) of 21% FiO₂, which were not affected by excessive oxygen, were given to the observer as the standard. The image series of other FiO₂ were randomly presented to the observer who was not aware of their FiO₂. The observer scored the degree of CSF hyperintensity artifact of the image series independently by comparing to those of 21% FiO₂. The assessment was conducted individually in six dogs. The degree of CSF SI increase in each image series was rated using a 4-point scale: none (0), mild (1), moderate (2), and severe (3) compared to the CSF SI of 21% FiO₂.

Statistical analyses

Statistical analyses were selected and conducted by one author with diagnostic imaging experience using a commercial software (IBM SPSS Statistics for Windows Version 25.0, SPSS Inc., Chicago, IL, USA). Spearman's rank correlation analysis was performed to demonstrate the correlation among FiO₂, PaO₂, and SI ratio of the seven CSF spaces and the normalizing regions. Friedman's test with Bonferroni's correction was used for assessing the SI ratios. *P*<0.05 was considered statistically significant. Intraobserver and interobserver reproducibility was assessed using the intraclass correlation coefficient, and a value close to 1 indicates excellent agreement.

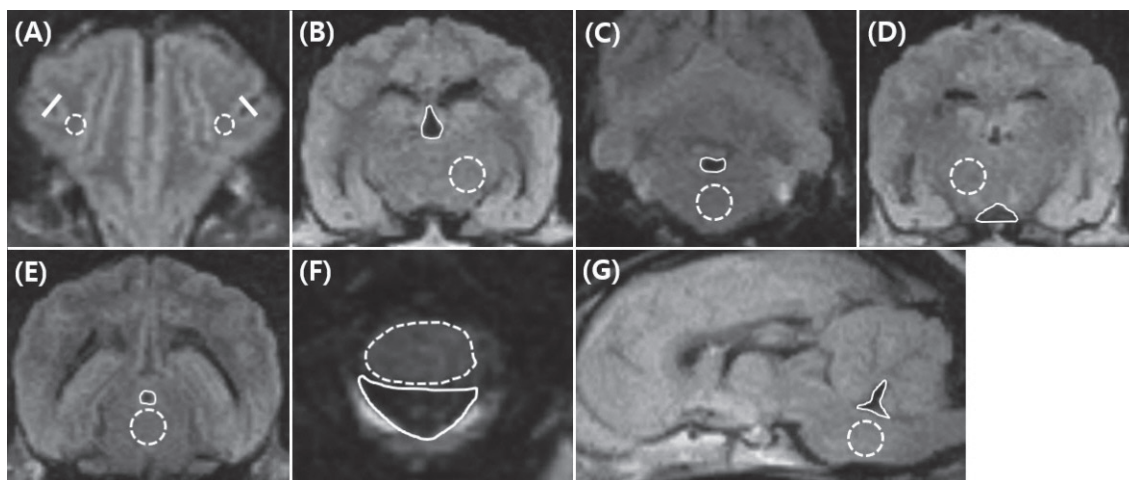


Fig. 1. Region of interest (ROI) shapes for signal intensity (SI) measurement marked in the transverse T2-weighted fluid attenuation inversion recovery (FLAIR) images of fraction of inspired oxygen (FiO₂) 21% at the level of frontal lobe (A), thalamus (B, D), pons (C), cerebral peduncle (E), C1 vertebra (F), and midsagittal plane (G). A, Linear ROIs for plot profile (solid lines) is arranged in the left and right coronal grooves, which exhibits a clear margin in the 21% FiO₂ image. Circular ROI of white matter for histogram analysis (circles of dotted line) is placed in the white matter adjacent to each coronal groove. Free hand ROI (solid lines) is drawn along the margin of each cerebrospinal fluid (CSF) spaces; 3rd ventricle (B), 4th ventricle (C, G), interpeduncular cistern (D), mesencephalic aqueduct (E), C1 subarachnoid space (F). Circular ROIs (circles of dotted line) were drawn in the normalizing regions; thalamus (B, D), pons (C, G), and cerebral peduncle (E). ROI of spinal cord was drawn in free hand due to its regular oval shape. Standard ROIs are selected and drawn in the 21% FiO₂ images with dark CSF spaces without the hyperintensity artifact because the margination becomes vague as the FiO₂ increases. The same shape and location of the ROI are applied to the images of other FiO₂ levels in each dog for measuring the SI. Slice thickness is 3 mm in all images.

RESULTS

Each dog underwent five FLAIR scans with different FiO_2 levels, and a total of 30 series of FLAIR sequences were obtained from the six dogs. All six dogs were included in the study because there was no abnormal finding in MRI scan, confirmed by subjective evaluation of three authors participated in the data analysis. Glycopyrrolate (5 $\mu\text{g}/\text{kg}$ IV, Morbinul[®], Seoul, Korea) was administered to regain the normal heart rate and blood pressure when 2 of the 6 dogs showed low blood pressure at the beginning of inhalation anesthesia. The results of CSF analysis were within the reference range in all dogs. The mean PaO_2 had a positive correlation with FiO_2 when analyzed using Spearman's rank correlation analysis, and low PaO_2 was observed in two dogs during the supply of 21% FiO_2 (Table 1).

Relatively larger CSF spaces, such as ventricles and cisterns, were observed in the 21% FiO_2 images obtained from all dogs, but not all of the cerebral sulci were clearly visible and some of the sulci had a vague margin. The mean SI ratio of the four data sets measured by two observers was acquired. The white matter, thalamus, pons, cerebral peduncle, and spinal cord were appropriate for normalization because the SI ratio of the regions had neither a positive nor negative correlation with FiO_2 (Table 2), indicating that the SI of those regions was not affected by the oxygen concentration. FiO_2 and the mean PaO_2 showed a positive correlation with the SI ratio of all CSF spaces (Table 3).

Significant differences were found in the SI ratio between 21% and 100% FiO_2 of all the selected CSF spaces ($P < 0.05$; Fig. 2). Five of the seven CSF spaces, namely sulci CSF spaces, third ventricle, interpeduncular cistern, subarachnoid space around the C1 spinal cord, and mesencephalic aqueduct, showed significant differences between the FLAIR images of 30% and 100% FiO_2 ($P < 0.05$). Moreover, 21% and 70% FiO_2 showed significant differences in the four spaces, namely cerebral sulci, third ventricle, interpeduncular cistern, and subarachnoid space of C1, and 50% and 100% FiO_2 had significant differences in only one CSF space ($P < 0.05$; Fig. 2). An agreement between two observers regarding the measurement of the SI ratio in the FLAIR images was good to excellent in seven CSF spaces (intraobserver 1: 0.733–0.977, intraobserver 2: 0.960–0.988, interobserver: 0.904–0.988).

In subjective evaluation, the mean score was 0.5 for 30% FiO_2 , 0.83 for 50% FiO_2 , 1.67 for 70% FiO_2 , and 2.67 for 100% FiO_2 .

Table 1. Values of the partial pressure of oxygen in arterial blood of six dogs according to the fraction of inspired oxygen (FiO_2) levels

FiO_2	PaO_2 (mmHg)	Dog 1	Dog 2	Dog 3	Dog 4	Dog 5	Dog 6
	Mean (\pm SD)						
21%	95.50 (\pm 29.58)	94	140	71 ^{a)}	66 ^{a)}	82	117
30%	158.83 (\pm 13.51)	179	139	153	165	154	163
50%	260.00 (\pm 12.95)	262	254	261	273	238	272
70%	354.67 (\pm 23.11)	342	371	356	389	323	347
100%	487.83 (\pm 32.30)	512	516	476	520	448	455

a) PaO_2 of Dog 3 and 4 in 21% FiO_2 was lower than normal range (80–100 mmHg¹⁴). SD, standard deviation. PaO_2 , partial pressure of arterial oxygen.

Table 2. Correlation analysis data of Spearman's rank correlation coefficient between fraction of inspired oxygen (FiO_2) and signal intensity (SI) ratio of normalizing region

FiO_2	White matter	Thalamus	Pons 1	Pons 2	Cerebral peduncle 1	Cerebral peduncle 2	Spinal cord
Spearman's rank correlation coefficient	-0.500	-0.800	0.000	-0.600	-0.300	0.100	0.300
Significance (2-tailed)	0.391	0.104	1.000	0.285	0.624	0.873	0.624

SI ratios of all normalizing regions are not correlated to FiO_2 (significance (2-tailed) $P > 0.05$), when analyzed by Spearman's rank correlation coefficient.

Table 3. Correlation analysis data of Spearman's rank correlation coefficient between fraction of inspired oxygen (FiO_2) and signal intensity (SI) ratio of cerebrospinal fluid (CSF) spaces, and between Mean partial pressure of arterial oxygen (PaO_2) and signal intensity (SI) ratio of CSF spaces

CSF spaces		Cerebral sulci	3rd ventricle	4th ventricle (transverse)	4th ventricle (midsagittal)	Interpeduncular cistern	Mesencephalic aqueduct	C1 subarachnoid space
FiO_2	Spearman's rank correlation coefficient	1.000	1.000	1.000	0.900	1.000	1.000	1.000
	Significance (2-tailed)	<0.001	<0.001	<0.001	0.037	<0.001	<0.001	<0.001
Mean PaO_2	Spearman's rank correlation coefficient	1.000	1.000	1.000	0.900	1.000	1.000	1.000
	Significance (2-tailed)	<0.001	<0.001	<0.001	0.037	<0.001	<0.001	<0.001

SI ratios of all CSF spaces are positively correlated to FiO_2 and also are positively correlated to Mean PaO_2 (significance (2-tailed) $P < 0.05$), when analyzed by Spearman's rank correlation coefficient.

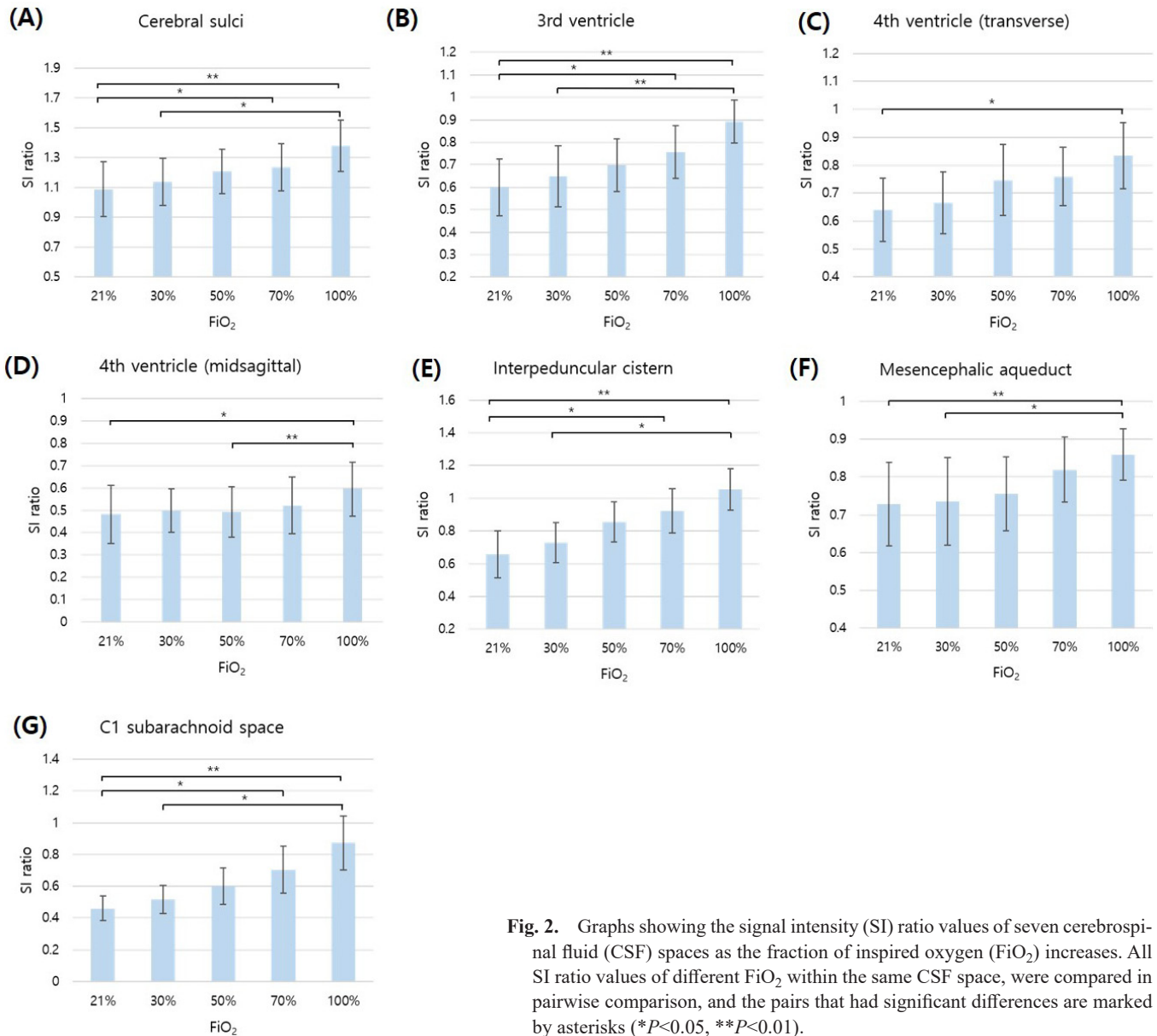


Fig. 2. Graphs showing the signal intensity (SI) ratio values of seven cerebrospinal fluid (CSF) spaces as the fraction of inspired oxygen (FiO₂) increases. All SI ratio values of different FiO₂ within the same CSF space, were compared in pairwise comparison, and the pairs that had significant differences are marked by asterisks (**P*<0.05, ***P*<0.01).

The artifact grade score increased with an increase in FiO₂. The score for 30% FiO₂ was close to 0, indicating no artifact, and the score for 100% FiO₂ was close to 3, indicating severe artifact (Fig. 3).

DISCUSSION

This study was performed to identify the highest FiO₂ that can reduce oxygen-induced hyperintensity in CSF spaces in the FLAIR sequence during MRI for anesthetized animals; this would allow the application of safe concentrations of oxygen during anesthesia for MRI and result in better FLAIR images. Veterinary radiologists may have difficulties in assessing oxygen-induced artifacts because they have been reading 100% FiO₂ images routinely as basic images. Therefore, 21% FiO₂ images which is same oxygen level of room air were provided as a standard for subjective evaluation. In this study, 21% FiO₂ is evaluated as inappropriate oxygen concentration because it might decrease patient's PaO₂ under normal range. FLAIR images obtained with 21% FiO₂ differed significantly from those obtained with 100% FiO₂, similar to the results of previous human studies [1, 3]. Images that differed significantly from the 21% FiO₂ images were noted to have the artifact, and those that differed significantly from the 100% FiO₂ images were noted to have no artifact. In addition, 70% FiO₂ was noted to induce the artifact because SI ratios were significantly increased in more than half of the CSF spaces. All six dogs maintained higher PaO₂ than normal under the 30% FiO₂ condition, and the artifact was not significant in both objective and subjective evaluations. Therefore, 30% FiO₂ was evaluated as the appropriate FiO₂ for reducing the occurrence of the oxygen-induced CSF hyperintensity artifact and for maintaining safe anesthesia.

Retrospective studies conducted in humans have reported that 50% FiO₂ or FiO₂ lower than 60% is less likely to induce an

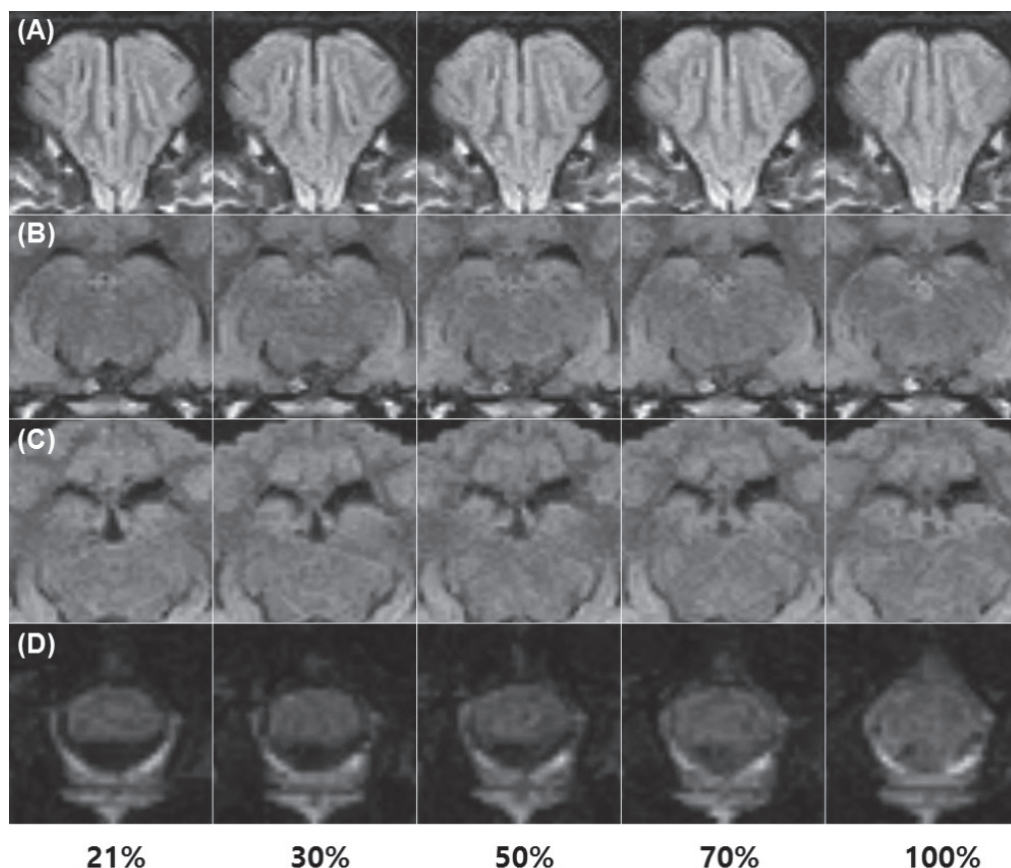


Fig. 3. Serial transverse T2-weighted fluid attenuation inversion recovery (FLAIR) images of the cerebrospinal fluid (CSF) spaces at the level of frontal lobe (A), cranial aspect of pons (B), thalamus (C), and C1 spinal cord (D). Bilateral coronal grooves (A), interpeduncular cistern (B), third ventricle (C), subarachnoid space at the C1 level (D) were selected as CSF space region of interest (ROI). The fraction of inspired oxygen (FiO_2) is 21%, 30%, 50%, 70% and 100% for the first, second, third, fourth, and fifth column of the figure, respectively. Increasing signal intensity (SI) and indistinctness are observed in the images with higher FiO_2 . Slice thickness is 3 mm in all images.

artifact [3, 4]. Consideration of these concentrations as accurate thresholds is difficult because there was only one patient who received 50% FiO_2 in the retrospective study [3], and 42.9% of 21 patients who received FiO_2 lower than 60% had marked hyperintensity in the cerebral sulcal subarachnoid space [4]. The difference between the suggested FiO_2 in humans and in dogs may be due to the different study designs or because intra-individual differences in oxygen concentration were not compared in the human study. Even if the studies are performed with the same methodology, there will be differences in threshold oxygen concentration between humans and animals because dogs and cats have a lower alveolar-arterial gradient and venous admixture [7].

The oxygenation effect varied by CSF space location in this study, for example, relatively narrow CSF space of cerebral sulci had more sensitive difference among FiO_2 levels, compared to the fourth ventricle. Several hypotheses were discussed in previous studies about this issue, thus human studies also had similar results. One study suggested that sulci have stronger hyperintensity because the oxygen is supplied into sulci subarachnoid space directly from much pial arterial vessels, while the ventricles do not have much blood vessel supply relative to the larger CSF volume [3]. Other study also agrees to the previous study, and assist that the greater volume of CSF per unit of pial vascularity will result in greater dilution of the oxygen, and will make the oxygen less effective [4]. Fourth ventricle SI ratio results of transverse and midsagittal plane were different. Partial volume artifact of CSF and surrounding cerebellum could have made the SI ratio less affected by oxygenation rather than difference of the plane. Possible inclusion of choroid plexus in the fourth ventricle ROI in midsagittal plane, could have affected to the SI ratio tendency.

The practical application of lowering the FiO_2 for veterinary patient needs careful consideration. Geriatric dogs and cats comprise a considerable portion of veterinary patients undergoing brain MRI, and patients with pulmonary dysfunction should also be administered general anesthesia if they need MRI. Older patients have less efficient oxygenation because of changes in pulmonary structures, blood flow, respiratory control, and reaction to drugs [7, 9, 21], and consequently, PaO_2 decreases with age for the same FiO_2 [7]. Respiratory diseases cause patients to be more vulnerable to hypoventilation during anesthesia and tend to lower the ventilation-perfusion (V/Q) ratio; thus, impairment of oxygenation can occur when patients receive low FiO_2 [7, 9]. The suggested 30% FiO_2 can be too low for these patients, and therefore, the individualized control of FiO_2 to obtaining a mean PaO_2 value (158.83 ± 13.51 mmHg), which corresponds to 30% FiO_2 in this study, can be alternative method.

The order of the FLAIR sequence among other MR sequences has to be decided before starting the MRI scan in order to apply the lowering FiO₂ technique. To minimize the risk of hypoxemia, the 30% FiO₂ can be administered only for the FLAIR sequence. Previous experimental and prospective studies performed the FLAIR sequence with 30% FiO₂ before or after other sequences, respectively, while 100% FiO₂ has been used for other sequences [4, 14]. The FLAIR sequence must be started after inhalation of lowered FiO₂ for at least 10 min to sufficiently decrease the P_{CSF}O₂, because the time in which the FiO₂ affects the P_{CSF}O₂ is approximately 10 min [10]. The FLAIR sequence is affected by T1 contrast medium, and thus, it has to be performed before the T1 contrast-enhanced sequence. If these two conditions are satisfied, the FLAIR sequence can be theoretically performed in any part of the protocol according to the needs of the patient.

False-positive misinterpretation has been reported in human FLAIR MRI [8]. Similarly, veterinary radiologists have to be careful of both false-positive and false negative misinterpretation, because all veterinary patients are anesthetized for MRI, and veterinary radiologists are accustomed to reading images obtained with 100% FiO₂. The FLAIR sequence has been reported to have superior diagnostic ability compared to gadolinium-enhanced T1-weighted MR for human subarachnoid space diseases [17]. Nonetheless, it is possible that previous studies could have included false-positive or false-negative results because some veterinary reports insist that the FLAIR sequence has limited diagnostic utility for meningeal diseases, provides no additional information, and detects occult brain lesions in relatively few patients [2, 11, 13].

Previous studies on the oxygen-induced hyperintensity artifact of the FLAIR sequence were all performed with the high-field MR scanner [1, 3–5, 14]. This artifact was expected to be less prevalent in low-field MR than in high-field MR because the paramagnetic effect of oxygen would be weaker with lower magnetic strength [14]. However, in this study, CSF hyperintensity was clearly observed in all six dogs when higher oxygen concentration was supplied in both objective and subjective evaluation. Furthermore, the FLAIR sequence has lower resolution compared to other sequences, and the low-field MR scanner has lower image quality than the high-field MR scanner owing to the reduced signal to noise ratio. Although high-field MR scanner is becoming popular in the veterinary sciences, low-field MR scanner will remain considerably prevalent owing to several advantages such as lower cost, safety, and greater patient accessibility [12]. Therefore, improving image quality in FLAIR and low-field MRI should be considered for general veterinary practice, and lowering FiO₂ can be one effort in this direction. In addition, various further studies related to the oxygen-induced CSF hyperintensity artifact have reported in humans; Using oxygen-induced hyperintensity in reverse, a noninvasive method of measuring P_{CSF}O₂ has been suggested [22]. In a recent study, magnetization-prepared 3D-FLAIR MRI has been investigated to eliminate the artifact [8]. Further studies should consider applying these techniques to animal patients.

The study had a few limitations. The expected level of proper FiO₂ was higher than the recommended minimal FiO₂ for general anesthesia (30% to 35%), but the selected oxygen level was similar to the minimal FiO₂ [7]. Five FiO₂ levels with 20% intervals were compared in this study; however, narrower oxygen-level intervals (5% or 10%) could have revealed a more specific FiO₂. Furthermore, the technique detailed in this study requires two flowmeters to control FiO₂ level, arterial catheterization, and a blood gas analyzer, which may restrict its practical applicability.

In conclusion, the oxygen-induced CSF hyperintensity artifact in FLAIR MR sequence does appear in low-field MRI with high FiO₂. Lowering FiO₂ can be used to remove this artifact; 30% FiO₂ was presumed to be the most appropriate oxygen concentration that can significantly reduce the oxygen-induced CSF hyperintensity artifact and maintain safe PaO₂.

REFERENCES

1. Anzai, Y., Ishikawa, M., Shaw, D. W., Artru, A., Yarnykh, V. and Maravilla, K. R. 2004. Paramagnetic effect of supplemental oxygen on CSF hyperintensity on fluid-attenuated inversion recovery MR images. *AJNR Am. J. Neuroradiol.* **25**: 274–279. [Medline]
2. Benigni, L. and Lamb, C. R. 2005. Comparison of fluid-attenuated inversion recovery and T2-weighted magnetic resonance images in dogs and cats with suspected brain disease. *Vet. Radiol. Ultrasound* **46**: 287–292. [Medline] [CrossRef]
3. Deliganis, A. V., Fisher, D. J., Lam, A. M. and Maravilla, K. R. 2001. Cerebrospinal fluid signal intensity increase on FLAIR MR images in patients under general anesthesia: the role of supplemental O₂. *Radiology* **218**: 152–156. [Medline] [CrossRef]
4. Frigon, C., Jardine, D. S., Weinberger, E., Heckbert, S. R. and Shaw, D. W. 2002. Fraction of inspired oxygen in relation to cerebrospinal fluid hyperintensity on FLAIR MR imaging of the brain in children and young adults undergoing anesthesia. *AJR Am. J. Roentgenol.* **179**: 791–796. [Medline] [CrossRef]
5. Frigon, C., Shaw, D. W., Heckbert, S. R., Weinberger, E. and Jardine, D. S. 2004. Supplemental oxygen causes increased signal intensity in subarachnoid cerebrospinal fluid on brain FLAIR MR images obtained in children during general anesthesia. *Radiology* **233**: 51–55. [Medline] [CrossRef]
6. Gavin, P. R. 2009. Physics. pp. 9, 23. In: *Practical Small Animal MRI* (Gavin, P. R. and Bagley, R. S.), John Wiley & Sons, New York.
7. Grimm, K. A., Lamont, L. A., Tranquilli, W. J., Greene, S. A. and Robertson, S. A. 2015. *Veterinary anesthesia and analgesia: The Fifth Edition of Lumb and Jones*. pp. 102, 543, 549, 989. John Wiley & Sons, Ames.
8. Jeong, H. K., Oh, S. W., Kim, J., Lee, S. K. and Ahn, S. J. 2016. Reduction of Oxygen-Induced CSF Hyperintensity on FLAIR MR Images in Sedated Children: Usefulness of Magnetization-Prepared FLAIR Imaging. *AJNR Am. J. Neuroradiol.* **37**: 1549–1555. [Medline] [CrossRef]
9. Kavanagh, B. P. and Hedenstierna, G. 2015. Respiratory physiology and pathophysiology. pp. 465–466. In: *Miller's Anesthesia*, 8th ed. (Miller, R. D. ed.), Saunders Elsevier, Philadelphia.
10. Kazemi, H., Klein, R. C., Turner, F. N. and Strieder, D. J. 1968. Dynamics of oxygen transfer in the cerebrospinal fluid. *Respir. Physiol.* **4**: 24–31. [Medline] [CrossRef]
11. Keenihan, E. K., Summers, B. A., David, F. H. and Lamb, C. R. 2013. Canine meningeal disease: associations between magnetic resonance imaging signs and histologic findings. *Vet. Radiol. Ultrasound* **54**: 504–515. [Medline] [CrossRef]
12. Konar, M. and Lang, J. 2011. Pros and cons of low-field magnetic resonance imaging in veterinary practice. *Vet. Radiol. Ultrasound* **52** Suppl 1: S5–S14. [Medline] [CrossRef]
13. Lamb, C. R., Croson, P. J., Cappello, R. and Cherubini, G. B. 2005. Magnetic resonance imaging findings in 25 dogs with inflammatory cerebrospinal

- fluid. *Vet. Radiol. Ultrasound* **46**: 17–22. [[Medline](#)] [[CrossRef](#)]
14. Moiola, M., Levionnois, O., Stein, V. M., Schüpbach, G., Schmidhalter, M. and Schweizer-Gorgas, D. 2017. Hyperintensity of cerebrospinal fluid on T2-weighted fluid-attenuated inversion recovery magnetic resonance imaging caused by high inspired oxygen fraction. *Front. Vet. Sci.* **4**: 219. [[Medline](#)] [[CrossRef](#)]
 15. Noguchi, K., Ogawa, T., Inugami, A., Toyoshima, H., Okudera, T. and Uemura, K. 1994. MR of acute subarachnoid hemorrhage: a preliminary report of fluid-attenuated inversion-recovery pulse sequences. *AJNR Am. J. Neuroradiol.* **15**: 1940–1943. [[Medline](#)]
 16. Robertson, I. 2011. Optimal magnetic resonance imaging of the brain. *Vet. Radiol. Ultrasound* **52** Suppl 1: S15–S22. [[Medline](#)] [[CrossRef](#)]
 17. Singer, M. B., Atlas, S. W. and Drayer, B. P. 1998. Subarachnoid space disease: diagnosis with fluid-attenuated inversion-recovery MR imaging and comparison with gadolinium-enhanced spin-echo MR imaging—blinded reader study. *Radiology* **208**: 417–422. [[Medline](#)] [[CrossRef](#)]
 18. Stuckey, S. L., Goh, T. D., Heffernan, T. and Rowan, D. 2007. Hyperintensity in the subarachnoid space on FLAIR MRI. *AJR Am. J. Roentgenol.* **189**: 913–921. [[Medline](#)] [[CrossRef](#)]
 19. Tha, K. K., Terae, S., Kudo, K. and Miyasaka, K. 2009. Differential diagnosis of hyperintense cerebrospinal fluid on fluid-attenuated inversion recovery images of the brain. Part II: non-pathological conditions. *Br. J. Radiol.* **82**: 610–614. [[Medline](#)] [[CrossRef](#)]
 20. Tsuchiya, K., Mizutani, Y. and Hachiya, J. 1996. Preliminary evaluation of fluid-attenuated inversion-recovery MR in the diagnosis of intracranial tumors. *AJNR Am. J. Neuroradiol.* **17**: 1081–1086. [[Medline](#)]
 21. Wahba, W. M. 1983. Influence of aging on lung function—clinical significance of changes from age twenty. *Anesth. Analg.* **62**: 764–776. [[Medline](#)] [[CrossRef](#)]
 22. Zaharchuk, G., Martin, A. J., Rosenthal, G., Manley, G. T. and Dillon, W. P. 2005. Measurement of cerebrospinal fluid oxygen partial pressure in humans using MRI. *Magn. Reson. Med.* **54**: 113–121. [[Medline](#)] [[CrossRef](#)]